Strengthening the adsorption performance of Cd(II) on sludge biochar by KMnO$_4$-modification

Weiwei Deng[a,b]

[a]*Civil & Architecture Engineering Institute, Zhengzhou University of Science and Technology, Zhengzhou 450000, China, email: zongqia184174@163.com*
[b]*Zhengzhou Regional Energy System Optimization Engineering Research Center, Zhengzhou 450000, China*

ABSTRACT

To enhance the Cd(II) adsorption capacity on sludge biochar (SBC), potassium permanganate modified sludge biochar (MSBC) was prepared. Additionally, the removal performance and adsorption behavior of Cd(II) on biochar were investigated by initial pH, coexisting ions, dosage, adsorption kinetics and adsorption isotherms. The Cd(II) adsorption behavior of SBC and MSBC was consistent with the pseudo-second-order kinetic model and the Langmuir model. The coexisting ion concentration of NaCl had almost no effect on the Cd(II) adsorption of SBC and MSBC. The maximum Cd(II) adsorption capacities of SBC and MSBC were 55.81 and 108.69 mg/g at the optimum conditions of 25°C, 1 g/L dosage and pH 5.0, respectively. After four replicate experiments, the removal efficiency of Cd(II) by SBC and MSBC was 64.05% and 90.34%, respectively. Complexation of Cd(II) with O-containing groups, Cd(II)-π interactions, co-precipitation and electrostatic interaction were the main mechanisms for the Cd(II) removal from aqueous solutions by SBC and MSBC. The KMnO$_4$-modification effectively enhanced the number of O-containing groups in the biochar and enhanced the complexation of Cd(II) by MSBC, which was the main reason for the increased Cd(II) adsorption capacity of MSBC. The results showed that KMnO$_4$-modification could effectively increase the Cd(II) adsorption by sludge biochar.

Keywords: Potassium permanganate modification; Sludge biochar; Cd(II); Adsorption performance; Mechanism

1. Introduction

With the rapid development of metal mining, smelting and processing and machinery manufacturing industries, large amounts of cadmium-containing wastewater are being discharged into the water environment and cadmium pollution has become a serious environmental problem [1]. In the natural environment, cadmium is non-degradable and can accumulate in living organisms, making it a more serious threat to the ecosystem [2]. Therefore, effective treatment of wastewater containing cadmium is essential. Currently, the main methods of treatment for cadmium-containing wastewater are chemical precipitation, electrochemical methods,

adsorption, ion exchange and membrane separation [3,4]. Among them, adsorption is the most promising technology for the treatment of heavy metal wastewater due to its simplicity, low-cost and high treatment efficiency [5].

For adsorption methods, the successful removal of pollutants depends on the choice of adsorbent with affinity for the target pollutant and fast adsorption rate [1]. Previous literature demonstrated that carbon-based materials (e.g., carbon nanotubes, graphene, biochar) are well suited as adsorbents for the treatment of heavy metal wastewater [1,2,6]. Of these, biochar has a very significant cost advantage, which makes it more promising for practical applications in heavy metal wastewater treatment. However,

biochar also suffers from relatively low adsorption capacity and poor adsorption selectivity for the removal of heavy metal ions [1,7,8]. Modification has been reported as one of the most effective ways to improve the adsorption performance of biochar for heavy metals [1]. The modification methods of biochar can be broadly classified into chemical modification, physical modification, mineral loading and magnetic modification [9]. Compared to other modification methods, chemical modification of $KMnO_4$ not only significantly improves the pore properties of biochar and increases the number of oxygen-containing functional groups, but also loads manganese oxides onto biochar, thus enhancing the interaction between biochar and heavy metal ions and more significantly improving the adsorption performance of biochar for heavy metals [1,10].

In this work, $KMnO_4$-modified sludge biochar was prepared to remove Cd(II) from aqueous solution. The main objectives of this work (1) to investigate the effect of $KMnO_4$-modification on the physicochemical properties of sludge biochar; (2) to explore the Cd(II) adsorption performance on biochar in terms of influencing factors (e.g., coexisting ions, dosage and solution pH), adsorption isotherms, and adsorption kinetics; (3) to analyze the potential mechanism of Cd(II) adsorption on biochar.

2. Materials and methods

2.1. Reagent and material

Cadmium nitrate ($Cd(NO_3)_2 \cdot 4H_2O$), nitric acid (HNO_3), sodium hydroxide (NaOH), sodium chloride (NaCl) and potassium permanganate ($KMnO_4$) were analytical reagent. All reagents were purchased from Sinopharm Reagent Group., Ltd., (Shanghai, China). Different concentrations of Cd(II) solution were prepared by dissolving different masses of $Cd(NO_3)_2 \cdot 4H_2O$ in deionized water.

2.1.1. Pre-treatment of dewatered sludge

Dewatered sludge from wastewater treatment plant in Zhengzhou (Henan Province, China). The sludge was transferred to a drying oven at 80°C and dried to a constant weight. The dried sludge was crushed into sludge powder and passed through an 80-mesh sieve. The sieved sludge powder was used for the preparation of sludge biochar.

2.2. Preparation of materials

2.2.1. Sludge biochar

The sludge powder was first placed in a tube furnace after passing N_2 for 1 h. The tube furnace was heated to 800°C at a rate of 20°C/min and N_2 was continuously introduced during the pyrolysis. The resulting biochar was recorded as sludge biochar (SBC).

2.2.2. $KMnO_4$ modified sludge biochar

2 g $KMnO_4$ was dissolved in 50 mL deionized water, 5 g SBC was added and shaken for 2 h in shaker, then filtered and dried. The black solid was noted as modified sludge biochar (MSBC).

2.3. Batch adsorption experiments

All adsorption experiments were performed in 50 mL polypropylene centrifuge tubes. The pH of the solution was adjusted with 0.01 mol/L HNO_3 or NaOH. The adsorption reaction was shaken on a rotary shaker at 150 rpm and 25°C. The effects of dosage (0.2~3.0 g/L), initial pH (2.0~7.0), coexisting ions concentration (0~0.1 mol/L) on Cd(II) removal were investigated.

After the reaction, the suspension was filtered through a 0.22 μm nylon membrane and the Cd(II) concentration in the filtrate was determined by atomic absorption spectrophotometry (Shimadzu, Model AA-6300, Japan). The removal efficiency [Eq. (1)] and the adsorption capacity [Eq. (2)] were calculated.

$$R(\%) = \frac{C_0 - C_e}{C_0} \times 100 \tag{1}$$

$$q = \frac{(C_0 - C_e) \times V}{m} \tag{2}$$

where R is the removal efficiency, %; C_0 is the initial Cd(II) concentration in solution, mg/L; C_e is the Cd(II) concentration in solution after adsorption equilibrium, mg/L; q is the equilibrium adsorption capacity, mg/g; V and m are the solution volume (mL) and adsorbent mass (mg), respectively.

2.3.1. Adsorption kinetics

The number of reactors required was designed according to a pre-designed time (5~300 min) interval. In each reactor, 25 mL of 10 mg/L Cd(II) solution was added to which 1 g/L of biochar was added and shaken at 25°C. The suspension was then removed at a pre-determined time and filtered to obtain the filtrate, which was measured for Cd(II) concentration. The pseudo-first-order model [Eq. (3)], the pseudo-second-order model [Eq. (4)] and the intraparticle diffusion model [Eq. (5)] were used for fitting analysis.

$$\ln(q_e - q_t) = \ln q_e - k_1 t \tag{3}$$

$$\frac{t}{q_t} = \frac{1}{1 + q_e^2 k_2} + \frac{t}{q_e} \tag{4}$$

$$q_t = K_d t^{1/2} + C_i \tag{5}$$

where q_e and q_t are the adsorption capacity at the equilibrium time and time "t" (mg/g), respectively; k_1 and k_2 represent adsorption rate constant of the pseudo-first-order (1/min) and the pseudo-second-order (g/mg·min), respectively; K_d (mg/(g·min$^{1/2}$)) is rate constants of intraparticle diffusion and film diffusion models; C_i is constant of the intraparticle diffusion model.

2.3.2. Adsorption isotherms

25 mL of Cd(II) solution with different concentrations (10~200 mg/L) was added to 1 g/L of biochar and the suspension was shaken at 25°C for 300 min. Then, the suspension

was filtered to obtain the filtrate and the Cd(II) concentration in the filtrate was determined. The Langmuir model [Eq. (6)] and Freundlich model [Eq. (7)] were used to fit this data.

$$q_e = \frac{q_{max}K_LC_e}{1+K_LC_e}, R_L = \frac{1}{1+K_LC_0} \qquad (6)$$

$$q_e = K_fC_e^{1/n} \qquad (7)$$

where q_e is the adsorption capacity at equilibrium (mg/g); C_e is the Cd(II) concentration at adsorption equilibrium (mg/L); q_{max}, K_L and R_L are the maximum Cd(II) adsorption capacity (mg/g), Langmuir equilibrium constant (L/mg) and separation factor, respectively; K_f and n represent the Freundlich affinity coefficient (mg^{1-n}·L^n/g) and Freundlich constant related to the surface site heterogeneity, respectively.

2.3.3. Repeatability experiments

The used adsorbent was mixed with 0.1 mol/L HCl solution, shaken at 25°C for 24 h, washed three times with deionized water and dried at 80°C for 24 h. The regenerated adsorbent was used for adsorption experiments.

2.4. Characterization methods

Scanning electron microscopy with energy-dispersive X-ray spectrometer (JSM-7500F, JEOL, Japan) was used to observe the microscopic morphology of the samples.

The crystalline structure and physical composition of the sample were analyzed using X-ray diffraction (XRD, D8X, Bruker, Germany). The surface chemical composition was analyzed with an X-ray photoelectron spectrometer (Escalab 250Xi, Thermo Fisher Scientific, USA) and Avantage software was used to perform peak splitting analysis. The Fourier-transform infrared spectrometer spectrum of biochar in the range of 4,000~500 cm^{-1} was determined by Fourier-transform infrared spectrometer (FTIR, Nicolet-460, Thermo Fisher, USA). The N$_2$ adsorption–desorption isotherm was analyzed by pore structure parameter (Tristar II Plus 2.02, USA), and the specific surface area, pore volume and pore size of biochar were analyzed. The amounts of O-containing functional groups (e.g., hydroxyl, carboxyl and lactone) in biochar were determined by Boehm titration [11].

3. Results and discussion

3.1. Physiochemical property analysis

The microstructures of SBC and MSBC are shown in Fig. 1. The SBC had a flat surface and there were no a large amount of particles on the surface. Moreover, the presence of element Mn was not detected in the energy-dispersive X-ray (EDS) spectrum of the SBC. Nevertheless, the MSBC surface (Fig. 1b) showed massive particles, and the element Mn appeared in EDS spectrum of MSBC, which indicated successful modification with potassium permanganate. The specific surface area, pore volume and pore size of SBC were 34.96 m²/g, 0.213 cm³/g and 11.36 nm, respectively.
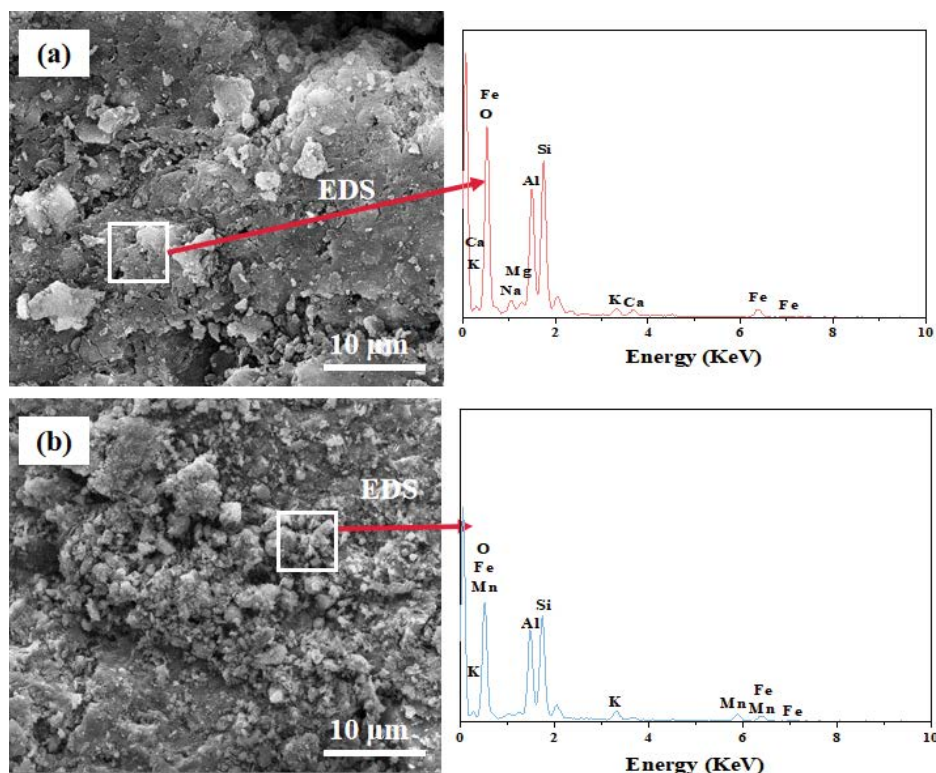

Fig. 1. Scanning electron microscopy with energy-dispersive X-ray spectroscopy analysis of sludge biochar (a) and modified sludge biochar (b).

However, the specific surface area, pore volume and pore size of MSBC were 64.29 m²/g, 0.278 cm³/g and 14.54 nm, respectively. The specific surface area, pore volume and pore size of MSBC were higher than those of SBC, signifying that MSBC could provide more adsorption sites for the Cd(II) removal [12]. Additionally, the amount of O-containing groups in the biochar was determined by titration. After KMnO₄-modification, the number of hydroxyl, carboxyl and lactone groups increased from 0.142, 0.176 and 0.039 to 0.213, 0.249 and 0.063 mmol/g. This indicated that the KMnO₄-modification increased the number of O-containing groups in the biochar, which provided more adsorption sites to remove Cd(II) from aqueous solution [11].

3.2. Effect of different factors on Cd(II) removal

3.2.1. Dosage

Fig. 2a shows the effect of dosage on the Cd(II) removal. As the dosage increased from 0.2 to 1 g/L, the Cd(II) removal efficiency by SBC and MSBC increased rapidly. This was because with the increase of dosage, the SBC and MSBC in the adsorption system can provide more adsorption sites for Cd(II), which was beneficial to the Cd(II) removal [7]. When the dosage was increased from 1 to 3 g/L, the Cd(II) removal efficiency by SBC and MSBC increased slowly. On the one hand, this was because the concentration of Cd(II) in the solution was limited [11]. On the other hand, an excessive dosage can cause agglomeration of the adsorbent, which in turn was not conducive to the diffusion of Cd(II) in the solution to its internal adsorption sites, thus leading to a slow increase in the removal efficiency [9]. Considering the removal efficiency and economic efficiency, the optimum dosage of adsorbent was 1 g/L.

3.2.2. Initial pH of solution

The removal performance of SBC and MSBC for Cd(II) at different initial pH is shown in Fig. 2b. As the initial pH increased, the removal efficiency of Cd(II) by SBC and MSBC showed an increasing trend, while this increasing trend became very slow when the initial pH was greater than 5.0. In general, the solution pH determined the surface charge of the adsorbent and the morphological distribution of pollutants in solution, which in turn affected the removal performance of pollutants by adsorbent [13]. The morphology of Cd(II) (at solution pH ≤ 8.0, Cd(II) was present in the form of Cd^{2+}) remained largely unchanged in the pH range of this work, which meant that the surface charge properties of SBC and MSBC was the main factor affecting the Cd(II) removal [14]. At low initial pH (pH of 2.0~3.0), the SBC and MSBC surfaces were highly protonated, resulting in electrostatic repulsion between the Cd^{2+} and adsorbents, making it difficult for them to diffuse onto the adsorbent surface [15]. At the same time, the competition between the large amount of H^+ and Cd^{2+} for the adsorption active sites on the SBC and MSBC surfaces was intense [8]. When the initial pH increased to the range of 4.0~5.0, the protonation of the SBC and MSBC surfaces decreased, resulting in a weaker electrostatic repulsion between them and Cd(II), and the reduced H^+ concentration also decreased

the competition with Cd(II) for the adsorption active sites, thus improving the adsorption efficiency of SBC and MSBC on Cd(II) [16]. When the initial pH is greater than 5.0, the liquid phase acidity gradually approached the pH_{ZPC} of SBC and MSBC, which theoretically increased the negative charge on the surface of adsorbent and enhanced the gravitational force between SBC and MSBC and Cd(II), improving the removal efficiency of Cd(II) [17]. In fact, the removal efficiency of Cd(II) was not significantly enhanced, probably because the Cd(II) binding site in SBC and MSBC was constant, which also indicated that electrostatic gravitational force was not a major role in the Cd(II) removal.

3.2.3. Coexisting ions

Fig. 2c shows the effect of ionic strength on the Cd(II) removal. The ionic strength was adjusted by adding a specific amount of NaCl to the solution. An increase in the ionic strength of solution had little effect on the Cd(II) adsorption by SBC and MSBC. This result suggested that Cd(II) adsorption followed specific chemisorption, as non-specific physical adsorption varies more for ionic strength than specific chemisorption [14,18].

3.2.4. Repeatability experiments

In 4 consecutive cycles experiments (Fig. 2d), the Cd(II) removal by SBC and MSBC gradually decreased during the cyclic adsorption process. After four cyclic experiments, the removal of Cd by SBC and MSBC was 64.05% and 90.34%, respectively. This may be due to the reduction in the active sites on the adsorbent surface after each cycle, which led to a reduction in the removal efficiency of Cd(II) [11]. However, the MSBC removal efficiency remained above 90% in the fourth cycle, indicating that the MSBC can be recycled several times.

3.3. Adsorption kinetics

The adsorption trends of SBC and MSBC for Cd(II) were approximately the same. During the initial stage of adsorption, the adsorption capacity of both biochar for Cd(II) increased rapidly due to the abundance of active sites on the adsorbent surface [4]. As the adsorption time increased, the effective active sites gradually decreased and the adsorption rate slowed down [14].

Adsorption kinetic models were used to evaluate the performance of adsorbents and to study the adsorption mechanism. To assess the adsorption kinetics process, data were fitted using pseudo-first-order kinetic, pseudo-second-order kinetic and intraparticle model. The pseudo-first-order kinetic model was based on the assumption that the adsorption process was physical, while the pseudo-second-order kinetic model assumed that the adsorption process was chemisorption [8]. The kinetic fitting results for the Cd(II) removal by SBC and MSBC are shown in Fig. 3 and Table 2. The results showed that the kinetics of Cd(II) removal followed the pseudo-first-order and pseudo-second-order kinetic models relatively well. However, the R^2 values of the pseudo-second-order kinetic model was relatively higher. The equilibrium adsorption capacities of Cd(II) by SBC and
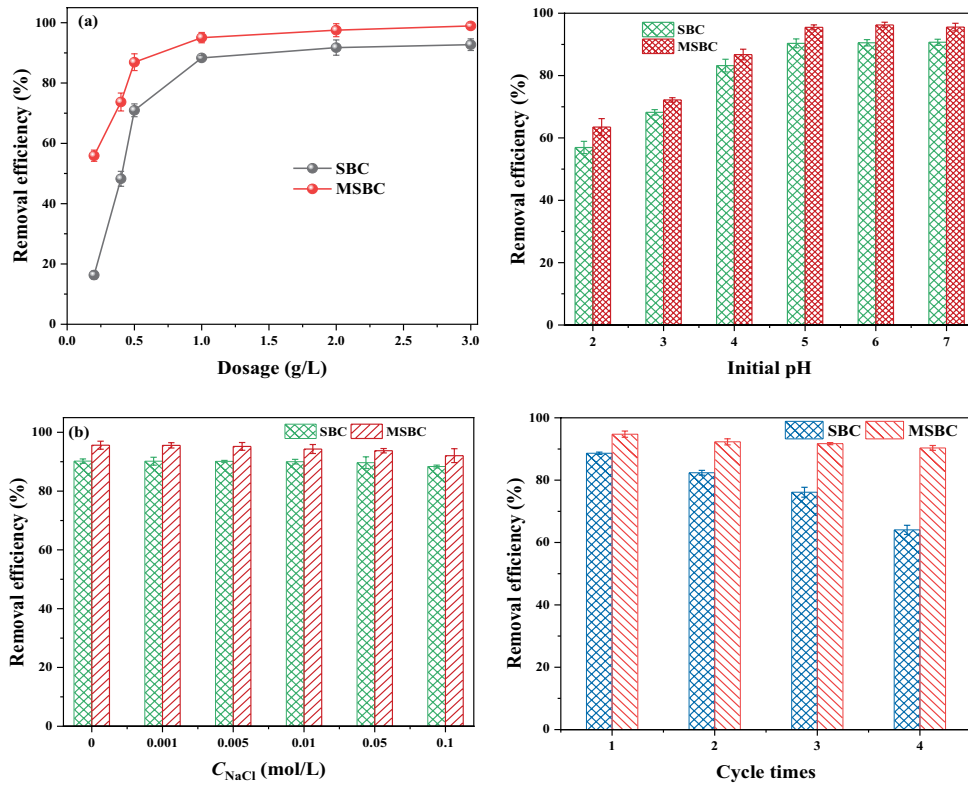
Fig. 2. Effect of dosage (a), initial pH (b), co-existing ions (c) and repeatability experiment (d) on the Cd(II) removal on sludge biochar and modified sludge biochar.
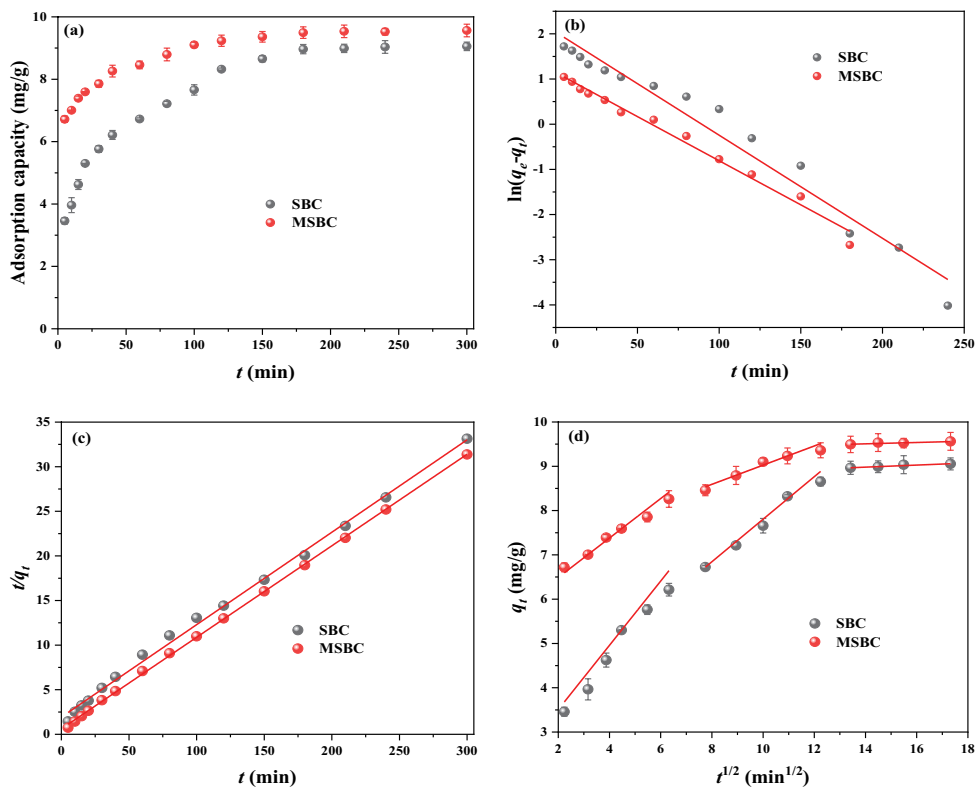

Fig. 3. Cd(II) adsorption capacity by sludge biochar and modified sludge biochar at various times (a). The pseudo-first-order (b), pseudo-second-order (c), and intraparticle diffusion (d) model fitting curve on the Cd(II) removal.

Table 1
Pore structure and O-containing functional numbers analysis of sludge biochar and modified sludge biochar

	Sludge biochar	Modified sludge biochar
Specific surface area (m²/g)	34.96	64.29
Pore volume (cm³/g)	0.213	0.278
Pore size (nm)	11.36	14.54
Hydroxyl (mmol/g)	0.142	0.213
Carboxylate (mmol/g)	0.176	0.249
Lactone (mmol/g)	0.039	0.063

Table 2
Kinetic model parameters of Cd(II) adsorption

		Sludge biochar	Modified sludge biochar
Pseudo-first-order	$q_{e,exp}$	9.05	9.56
	$q_{e,cal}$	7.68	3.14
	k_1	0.023	0.020
	R^2	0.961	0.985
Pseudo-second-order	$q_{e,cal}$	9.04	9.76
	k_2	0.006	0.017
	R^2	0.997	0.999
Intraparticle model	K_{d1}	0.725	0.446
	C_1	2.06	5.60
	R_1^2	0.942	0.998
	K_{d2}	0.480	0.217
	C_2	3.00	6.86
	R_2^2	0.991	0.928
	K_{d3}	0.023	0.015
	C_3	8.656	9.30
	R_3^2	0.950	0.917

MSBC obtained from the pseudo-second-order kinetic model were 9.04 and 9.76 mg/g, respectively, which were less different from the experimental results ($q_{e,exp}$). This suggested that the Cd(II) removal by SBC and MSBC was controlled by chemisorption (i.e., chemical bonds may be formed between Cd(II) and the adsorbent by sharing or exchanging electrons) [9].

From the mass transfer process, the Cd(II) removal was divided into 3 stages: the fast adsorption stage (0~60 min), the slow adsorption stage (60~120 min) and the adsorption equilibrium stage (120~300 min). In stage 1, due to the high Cd(II) concentration difference between the liquid phase and the adsorbent surface, Cd(II) diffused rapidly across the liquid film to the adsorbent surface and bound to a large number of effective adsorption sites on its surface, where liquid film diffusion and surface adsorption occurred [11]. In stage 2, the Cd(II) diffusing to the adsorbent surface decreased as the concentration difference between the solid and liquid phases decreased. As the effective adsorption sites on the adsorbent surface decreased, the Cd(II) adsorbed on the surface gradually diffused into the pores (intraparticle

diffusion) and underwent pore filling [3]. In stage 3, with the further reduction of the concentration difference between the solid and liquid phases and the gradual saturation of the effective adsorption sites, the whole system showed a dynamic equilibrium [19]. The R^2 values of both liquid film diffusion and the intraparticle diffusion model were within acceptable limits, and the values of C_1 and C_2 were not zero, indicating that the removal rate of Cd(II) was determined by both liquid film diffusion and intraparticle diffusion [19]. Meanwhile, the values of K_d in stage 1 were much higher than those in stages 2 and 3, indicating that liquid film diffusion was the rate-controlling step for Cd(II) removal [11].

3.4. Adsorption isotherms

As shown in Fig. 4, the adsorption capacity of Cd(II) by biochar first increased gradually and then saturated. At low concentrations, Cd(II) was almost completely adsorbed. After increasing the Cd(II) concentration, it was found that the adsorption capacity basically did not change much and finally remained in a stable state of adsorption. This was because at low concentration solutions, the biochar provided a large number of attachment sites and functional groups, but as the solution concentration continued to increase, the attachment sites were gradually filled, and the functional groups were occupied [5]. Additionally, the adsorption capacity of MSBC was higher than that of SBC at the same adsorption temperature. Notably, increasing the temperature could facilitate the Cd(II) removal by biochar [13].

Adsorption isotherm models were used to predict the adsorption equilibrium mechanism, adsorption capacity and inherent properties of the adsorption process, and were an important method for evaluating the adsorption performance. The results of Langmuir and Freundlich models are shown in Fig. 4 and Table 3. The Langmuir model assumes that the adsorbent surface is homogeneous, and adsorption occurs on the molecular surface layer [18]. The Freundlich model is applied to the adsorption on inhomogeneous surfaces [7]. In the Cd(II) adsorption, the Langmuir model had a better fit for Cd(II) adsorption by SBC and MSBC, with fit coefficients higher than 0.96 and 0.97, respectively, indicating that the Cd(II) adsorption by SBC and MSBC was dominated by monolayer adsorption [5]. In addition, the results of the Langmuir model fit showed that the maximum adsorption capacities of SBC and MSBC for Cd(II) were 55.81 and 108.69 mg/g, respectively, and the maximum adsorption capacity of MSBC was increased by 94.75% compared to SBC. The K_L and q_e of Langmuir model increased with increasing reaction temperature, indicating that both the bonding energy and electron transfer capacity between the adsorption site and Cd(II) were enhanced [18]. Therefore, SBC and MSBC had better Cd(II) adsorption potential at high temperatures. Meanwhile, the separation factor (R_L) of the Langmuir model remained between 0 and 1, indicating that the whole adsorption process was favorable [11].

3.5. Mechanistic analysis

The functional groups of the biochar were identified by FTIR (Fig. 5a). The wavenumber at 3,430 and 1,630 cm⁻¹ correspond to O–H stretching vibrations and C=C stretching
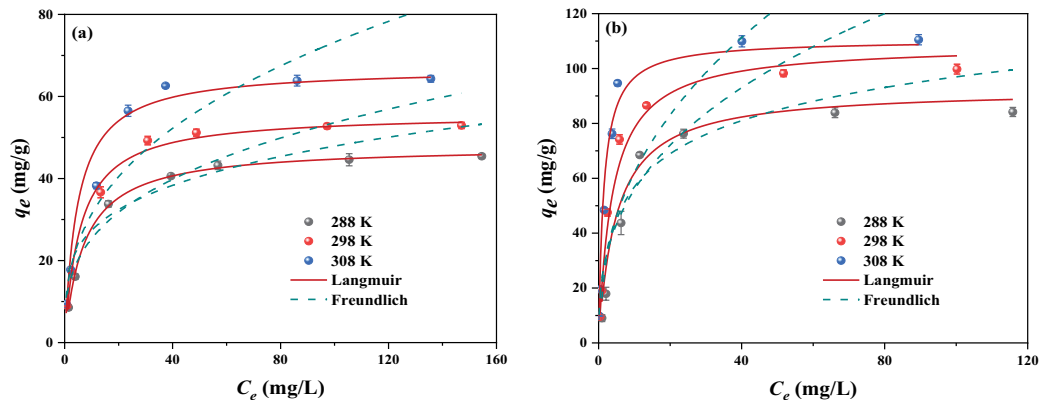
Fig. 4. Isothermal model fitting of Cd(II) adsorption on sludge biochar (a) and modified sludge biochar (b).

Table 3
Isotherm model parameters of Cd(II) adsorption

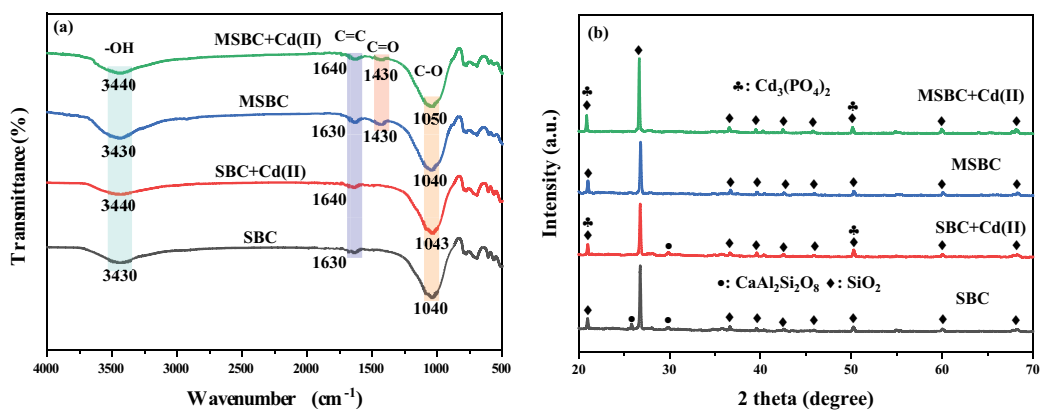|		Sludge biochar			Modified sludge biochar		
		288	298	308	288	298	308
Langmuir	q_{max}	47. 91	55.81	66.96	92.53	108.69	110.43
	K_L	0. 140	0.173	0.209	0.202	0.57	0.700
	R_L	0.087	0.081	0.076	0.077	0.051	0.048
		~0.417	~0.367	~0.323	~0.332	~0.149	~0.125
	R^2	0.998	0.993	0.968	0.972	0.993	0.978
Freundlich	K_f	15.64	11.98	13.41	15.61	23.94	23.51
	n	4.12	3.07	2.71	1.34	2.72	2.37
	R^2	0.805	0.925	0.912	0.870	0.818	0.708

Fig. 5. Fourier-transform infrared spectroscopy (a) and X-ray diffraction (b) analysis of adsorbent before and after Cd(II) adsorption.

vibrations present in SBC and MSBC, respectively [18]. In addition, the wavenumber at 1,040 cm⁻¹ corresponds to the C–O vibrational peak in the SBC and MSBC [12]. Of note was the enhancement of the stretching vibrational peak of –OH in MSBC after modification, which indicated an increase in the content of –OH in MSBC [15]. This result was consistent with previous findings that the content of –OH groups on biochar increased after KMnO₄-modification [3]. Notably, new characteristic peak of C=O in carboxyl or carbonyl groups located at 1,430 cm⁻¹ was also observed in the MSBC, indicating that more O-containing groups were generated from the biochar after modification with potassium permanganate [14]. After Cd(II) adsorption, the –OH stretching vibrations of SBC and MSBC at 3,430 cm⁻¹ were shifted to 3,440 cm⁻¹, indicating that the hydroxyl functional groups in SBC and MSBC were involved in the adsorption [9]. In addition, the C–O group was similarly shifted after adsorption. The C=O peaks of the carboxyl or carbonyl groups in MSBC were attenuated after adsorption [6]. The above evidence suggested that complexation between O-containing
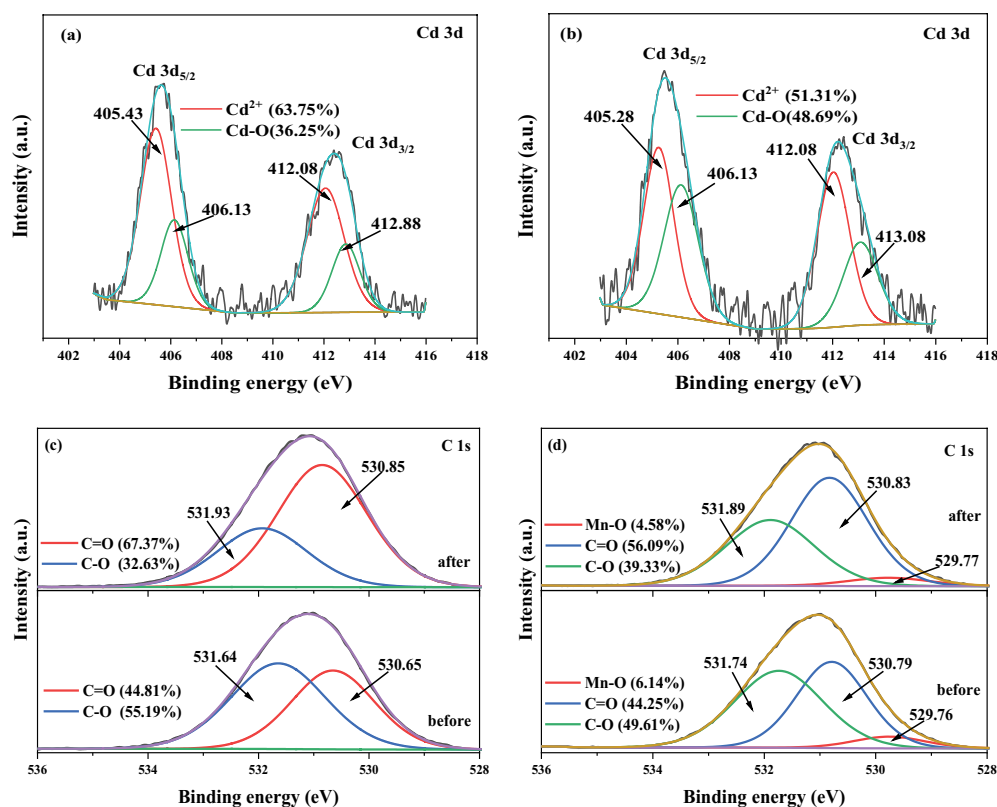
Fig. 6. X-ray photoelectron spectra of Cd 3d and C 1s before and after Cd(II) adsorption on sludge biochar (a and c) and modified sludge biochar (b and d).

groups (e.g., hydroxyl, carboxyl and carbonyl groups) in biochar and Cd(II) occurred [4]. The C=C groups in SBC and MSBC were shifted to 1,640 cm^{-1} after adsorption and the intensity of C=C groups was diminished. According to previous literature, this could be due to a cation-π interaction between the C=C groups in the biochar and Cd(II) [11].

The phase composition and crystalline structure of SBC and MSBC were analyzed by XRD (Fig. 5b). The main characteristic peak in SBC and MSBC was identified as silica (PDF. # 46-1045) [20]. Additionally, the CaAl$_2$Si$_2$O$_8$ (PDF. # 20-0452) was appeared in the SBC [9]. However, the diffraction patterns of SBC and MSBC were similar and no MnO$_x$ peaks were detected in the Mn-containing MSBC. This may be due to the low content of crystalline MnO$_x$ or their presence as a disordered phase [13,16]. In the adsorbed SBC and MSBC, there was a significant enhancement of the intensity of the characteristic peaks at 2θ of 20.82° and 50.29°, presumably due to the precipitation of cadmium phosphate (PDF. # 31-0234) on the surface of the SBC and MSBC [18].

The characteristic peak of Cd 3d is displayed in Fig. 6a and b. The main forms of Cd(II) were Cd^{2+} and Cd–O. Previous studies have shown that Cd^{2+} represented cadmium precipitations, while the Cd–O may be due to complexation between Cd(II) and the O-containing functional groups on the adsorbent [21]. The relative contents of Cd^{2+} and Cd–O in SBC were 63.75% and 36.25%, respectively. Notably, the amount of Cd–O in the MSBC was 48.69%, while the amount of Cd^{2+} was only 51.31%. This also indicated that the KMnO$_4$-modification could enhance the complexation ability of

MSBC towards Cd(II) [17]. To further illustrate the complexation reaction of the O-containing groups in the adsorbent for the Cd(II) adsorption in aqueous solution [8]. Fig. 6c and d show the O 1s fine spectra of SBC and MSBC before and after the adsorption of Cd(II), respectively. The O 1s of SBC was divided into C=O and C–O characteristic peaks [11]. Notably, a smaller M–O peak (529.76 eV) was displayed in the O 1s of MSBC, indicating that the manganese oxides were successfully loaded on MSBC [17]. After adsorption, the binding energies of the C=O and C–O characteristic peaks in both SBC and MSBC showed an increase. Moreover, the relative contents of C=O and C–O showed an increase and a decrease, respectively. These findings confirmed the complexation of the O-containing groups in the biochar with Cd(II) [4]. This was also consistent with previous studies. Notably, the binding energy of M–O also showed an increase after adsorption, which may also be involved in the Cd(II) adsorption [17].

In summary, the mechanism of Cd(II) adsorption included: (1) complexation with O-containing groups; (2) Cd(II)-π interaction of C=C groups with Cd(II); (3) co-precipitation between phosphates released by biochar and Cd(II); (4) electrostatic interaction.

4. Conclusion

Overall, the KMnO$_4$-modification increased the number of O-containing groups in the biochar thus enhancing the adsorption capacity of modified biochar for

Cd(II). The maximum adsorption capacity of Cd(II) on MSBC (108.69 mg/g) was approximately twice that of SBC (55.81 mg/g) at 25°C. The adsorption behavior of Cd(II) on SBC and MSBC was spontaneous, heat-absorbing and homogeneous chemisorption. After four replicate experiments, the removal efficiency of Cd(II) on SBC and MSBC was 64.05% and 90.34%, respectively. Complexation of Cd(II) with O-containing groups, Cd-π interaction, co-precipitation and electrostatic interaction were the main mechanisms for the removal of Cd(II) from aqueous solutions by SBC and MSBC. The results of this work indicated that $KMnO_4$-modification could improve the Cd(II) removal capacity of sludge biochar and provide a theoretical basis for the removal of actual Cd(II)-containing wastewater.

Funding

Conflicts of interest

The authors declare that we have no competing financial interests.

References

[1] S.M. Shaheen, Natasha, A. Mosa, A. El-Naggar, Md Faysal Hossain, H. Abdelrahman, N. Khan Niazi, M. Shahid, T. Zhang, Y. Fai Tsang, L. Trakal, S.S. Wang, J. Rinklebe, Manganese oxide-modified biochar: production, characterization and applications for the removal of pollutants from aqueous environments - a review, Bioresour. Technol., 346 (2022) 126581, doi: 10.1016/j.biortech.2021.126581.

[2] K. Zhang, Y.Q. Yi, Z.Q. Fang, Remediation of cadmium or arsenic contaminated water and soil by modified biochar: a review, Chemosphere, 311 (2023) 136914, doi: 10.1016/j.chemosphere.2022.136914.

[3] S. Chen, M. Zhong, H. Wang, S. Zhou, W. Li, T. Wang, J. Li, Study on adsorption of Cu^{2+}, Pb^{2+}, Cd^{2+}, and Zn^{2+} by the $KMnO_4$ modified biochar derived from walnut shell, Int. J. Environ. Sci. Technol., 20 (2022) 1551–1568.

[4] X.J. Chen, Q.M. Lin, H.Y. Xiao, R. Muhammad, Manganese-modified biochar promotes Cd accumulation in *Sedum alfredii* in an intercropping system, Environ. Pollut., 317 (2023) 120525, doi: 10.1016/j.envpol.2022.120525.

[5] P. Fu, X. Wang, J. Shi, L.X. Zhou, Q.J. Hou, W.Q. Wang, Y. Tian, J.M. Qin, W.L. Bi, F.W. Liu, Enhanced removal of As(III) and Cd(II) from wastewater by alkali-modified Schwertmannite@ Biochar, Environ. Technol. Innovation, 31 (2023) 103197, doi: 10.1016/j.eti.2023.103197.

[6] Z.Y. Feng, N. Chen, T. Liu, C.P. Feng, $KHCO_3$ activated biochar supporting MgO for Pb(II) and Cd(II) adsorption from water: experimental study and DFT calculation analysis, J. Hazard. Mater., 426 (2022) 128059, doi: 10.1016/j.jhazmat.2021.128059.

[7] H.Y. Wang, B. Gao, S.S. Wang, J.N. Fang, Y.W. Xue, K. Yang, Removal of Pb(II), Cu(II), and Cd(II) from aqueous solutions by biochar derived from $KMnO_4$ treated hickory wood, Bioresour. Technol., 197 (2015) 356–362.

[8] P. Wu, P.X. Cui, Y. Zhang, M.E. Alves, C. Liu, D.M. Zhou, Y.J. Wang, Unraveling the molecular mechanisms of Cd sorption onto MnO_x-loaded biochar produced from the Mn-hyperaccumulator *Phytolacca americana*, J. Hazard. Mater., 423 (2022) 127157, doi: 10.1016/j.jhazmat.2021.127157.

[9] M.Y. Jiang, R.X. Chen, B.Y. Cao, F. Wang, The performance of temperature and acid-modified sludge in removing lead and cadmium, Environ. Sci. Pollut. Res., 30 (2023) 76072–76084.

[10] X. Yin, Y.L. Wang, L.E. Wei, H.J. Huang, C.H. Zhou, G.R. Ni, Reduced cadmium(Cd) accumulation in lettuce plants by applying $KMnO_4$ modified water hyacinth biochar, Heliyon, 8 (2022) e11304, doi: 10.1016/j.heliyon.2022.e11304.

[11] B. Li, L. Yang, C.Q. Wang, Q.P. Zhang, Q.C. Liu, Y.D. Li, R. Xiao, Adsorption of Cd(II) from aqueous solutions by rape straw biochar derived from different modification processes, Chemosphere, 175 (2017) 332–340.

[12] J.Z. Zhang, X.F. Ma, L. Yuan, D.X. Zhou, Comparison of adsorption behavior studies of Cd^{2+} by vermicompost biochar and $KMnO_4$-modified vermicompost biochar, J. Environ. Manage., 256 (2020) 109959, doi: 10.1016/j.jenvman.2019.109959.

[13] X.Q. Liu, D.D. Li, J.G. Li, J.L. Wang, S.J. Liang, H. Deng, A novel MnO_x-impregnated on peanut shells derived biochar for high adsorption performance of Pb(II) and Cd(II): behavior and mechanism, Surf. Interfaces, 34 (2022) 102323, doi: 10.1016/j.surfin.2022.102323.

[14] C. Sun, T. Chen, Q.X. Huang, J. Wang, S.Y. Lu, J.H. Yan, Enhanced adsorption for Pb(II) and Cd(II) of magnetic rice husk biochar by $KMnO_4$ modification, Environ. Sci. Pollut. Res., 26 (2019) 8902–8913.

[15] G.C. Yin, X.L. Chen, B. Sarkar, N.S. Bolan, T. Wei, H.Y. Zhou, H.L. Wang, Co-adsorption mechanisms of Cd(II) and As(III) by an Fe-Mn binary oxide biochar in aqueous solution, Chem. Eng. J., 466 (2023) 143199, doi: 10.1016/j.cej.2023.143199.

[16] H.S. Lee, H.S. Shin, Competitive adsorption of heavy metals onto modified biochars: comparison of biochar properties and modification methods, J. Environ. Manage., 299 (2021) 113651, doi: 10.1016/j.jenvman.2021.113651.

[17] H.S. Lee, Y. Kim, J. Kim, H.S. Shin, Quantitative and qualitative characteristics of dissolved organic matter derived from biochar depending on the modification method and biochar type, J. Water Process Eng., 46 (2022) 102569, doi: 10.1016/j.jwpe.2022.102569.

[18] W.L. Wu, Z.H. Liu, M. Azeem, Z.Q. Guo, R.H. Li, Y.G. Li, Y.R. Peng, E.F. Ali, H.L. Wang, S.S. Wang, J. Rinklebe, S.M. Shaheen, Z.Q. Zhang, Hydroxyapatite tailored hierarchical porous biochar composite immobilized Cd(II) and Pb(II) and mitigated their hazardous effects in contaminated water and soil, J. Hazard. Mater., 437 (2022) 129330, doi: 10.1016/j.jhazmat.2022.129330.

[19] K.W. Jung, S.Y. Lee, J.W. Choi, Y.J. Lee, A facile one-pot hydrothermal synthesis of hydroxyapatite/biochar nanocomposites: adsorption behavior and mechanisms for the removal of copper(II) from aqueous media, Chem. Eng. J., 369 (2019) 529–541.

[20] M.L. Wu, B. Liu, J. Li, X.T. Su, W.Z. Liu, X.Q. Li, Influence of pyrolysis temperature on sludge biochar: the ecological risk assessment of heavy metals and the adsorption of Cd(II), Environ. Sci. Pollut. Res., 30 (2023) 12608–12617.

[21] J.W. Wu, T. Wang, J.W. Wang, Y.S. Zhang, W.P. Pan, A novel modified method for the efficient removal of Pb and Cd from wastewater by biochar: enhanced the ion exchange and precipitation capacity, Sci. Total Environ., 754 (2021) 142150, doi: 10.1016/j.scitotenv.2020.142150.